J|A|C|S
ARTICLES
Published on Web 02/02/2006

Specific and Stable Fluorescence Labeling of Histidine-Tagged Proteins for Dissecting Multi-Protein Complex Formation

Suman Lata, Martynas Gavutis, Robert Tampé, and Jacob Piehler*

Contribution from the Institut für Biochemie, Johann Wolfgang Goethe-University, Biozentrum N210, Marie-Curie-Strasse 9, D-60439 Frankfurt am Main, Germany

Received September 13, 2005; E-mail: j.piehler@em.uni-frankfurt.de

Abstract: Labeling of proteins with fluorescent dyes offers powerful means for monitoring protein interactions in vitro and in live cells. Only a few techniques for noncovalent fluorescence labeling with well-defined localization of the attached dye are currently available. Here, we present an efficient method for site-specific and stable noncovalent fluorescence labeling of histidine-tagged proteins. Different fluorophores were conjugated to a chemical recognition unit bearing three NTA moieties (tris-NTA). In contrast to the transient binding of conventional mono-NTA, the multivalent interaction of tris-NTA conjugated fluorophores with oligohistidine-tagged proteins resulted in complex lifetimes of more than an hour. The high selectivity of tris-NTA toward cumulated histidines enabled selective labeling of proteins in cell lysates and on the surface of live cells. Fluorescence labeling by tris-NTA conjugates was applied for the analysis of a ternary protein complex in solution and on surfaces. Formation of the complex and its stoichiometry was studied by analytical size exclusion chromatography and fluorescence quenching. The individual interactions were dissected on solid supports by using simultaneous mass-sensitive and multicolor fluorescence detection. Using these techniques, formation of a 1:1:1 stoichiometry by independent interactions of the receptor subunits with the ligand was shown. The incorporation of transition metal ions into the labeled proteins upon labeling with tris-NTA fluorophore conjugates provided an additional sensitive spectroscopic reporter for detecting and monitoring protein−protein interactions in real time. A broad application of these fluorescence conjugates for protein interaction analysis can be envisaged.

Introduction

One of the key challenges in life science research in the coming years is the identification and characterization of protein−protein interactions and multi-protein complexes. Proteome-wide dissection and biophysical characterization of protein−protein interaction networks requires simple and generic techniques for attaching spectroscopic probes on proteins. Fluorescent probes are particularly powerful for the detection of protein−protein interactions providing highly sensitive and versatile read-outs such as fluorescence resonance energy transfer (FRET), fluorescence anisotropy, or fluorescence correlation spectroscopy.[1−4] Despite the tremendous success of autofluorescent proteins and the large variety of currently available species,[5] techniques for site-specific labeling of proteins with synthetic fluorophores are currently gaining importance because these approaches offer even broader choices of fluorophores and more flexible applications.[6−8] While several techniques for site-specific covalent coupling of fluorophores are available,[9−16] reversible attachment by noncovalent interaction further enhances the versatility of labeling.[6,17−22] Ideal noncovalent fluorescence labeling unites specific, stable, and stoichiometric attachment with the possibility for rapidly removing the label. Such switchable labeling has not yet been

(1) Miyawaki, A.; Tsien, R. Y. *Methods Enzymol.* **2000**, *327*, 472−500.
(2) Yan, Y.; Marriott, G. *Curr. Opin. Chem. Biol.* **2003**, *7*, 635−640.
(3) Pramanik, A. *Curr. Pharm. Biotechnol.* **2004**, *5*, 205−212.
(4) Clayton, A. H.; Hanley, Q. S.; Arndt-Jovin, D. J.; Subramaniam, V.; Jovin, T. M. *Biophys. J.* **2002**, *83*, 1631−1649.
(5) Miyawaki, A.; Sawano, A.; Kogure, T. *Nat. Cell Biol.* **2003**, Suppl., S1−7.
(6) Chen, I.; Ting, A. Y. *Curr. Opin. Biotechnol.* **2005**, *16*, 35−40.
(7) Johnsson, N.; Johnsson, K. *Chembiochem* **2003**, *4*, 803−810.
(8) Zhang, J.; Campbell, R. E.; Ting, A. Y.; Tsien, R. Y. *Nat. Rev. Mol. Cell Biol.* **2002**, *3*, 906−918.
(9) Griffin, B. A.; Adams, S. R.; Tsien, R. Y. *Science* **1998**, *281*, 269−272.
(10) Keppler, A.; Gendreizig, S.; Gronemeyer, T.; Pick, H.; Vogel, H.; Johnsson, K. *Nat. Biotechnol.* **2003**, *21*, 86−89.
(11) Yin, J.; Liu, F.; Li, X.; Walsh, C. T. *J. Am. Chem. Soc.* **2004**, *126*, 7754−7755.
(12) Wood, R. J.; Pascoe, D. D.; Brown, Z. K.; Medlicott, E. M.; Kriek, M.; Neylon, C.; Roach, P. L. *Bioconjugate Chem.* **2004**, *15*, 366−372.
(13) George, N.; Pick, H.; Vogel, H.; Johnsson, N.; Johnsson, K. *J. Am. Chem. Soc.* **2004**, *126*, 8896−8897.
(14) Adams, S. R.; Campbell, R. E.; Gross, L. A.; Martin, B. R.; Walkup, G. K.; Yao, Y.; Llopis, J.; Tsien, R. Y. *J. Am. Chem. Soc.* **2002**, *124*, 6063−6076.
(15) Chen, I.; Howarth, M.; Lin, W.; Ting, A. Y. *Nat. Methods* **2005**, *2*, 99−104.
(16) Zhang, Z.; Smith, B. A.; Wang, L.; Brock, A.; Cho, C.; Schultz, P. G. *Biochemistry* **2003**, *42*, 6735−6746.
(17) Wu, M. M.; Llopis, J.; Adams, S.; McCaffery, J. M.; Kulomaa, M. S.; Machen, T. E.; Moore, H. P.; Tsien, R. Y. *Chem. Biol.* **2000**, *7*, 197−209.
(18) Kapanidis, A. N.; Ebright, Y. W.; Ebright, R. H. *J. Am. Chem. Soc.* **2001**, *123*, 12123−12125.
(19) Miller, L. W.; Sable, J.; Goelet, P.; Sheetz, M. P.; Cornish, V. W. *Angew Chem., Int. Ed.* **2004**, *43*, 1672−1675.
(20) Guignet, E. G.; Hovius, R.; Vogel, H. *Nat. Biotechnol.* **2004**, *22*, 440−444.
(21) Miller, L. W.; Cai, Y.; Sheetz, M. P.; Cornish, V. W. *Nat. Methods* **2005**, *2*, 255−257.
(22) Miller, L. W.; Cornish, V. W. *Curr. Opin. Chem. Biol.* **2005**, *9*, 56−61.

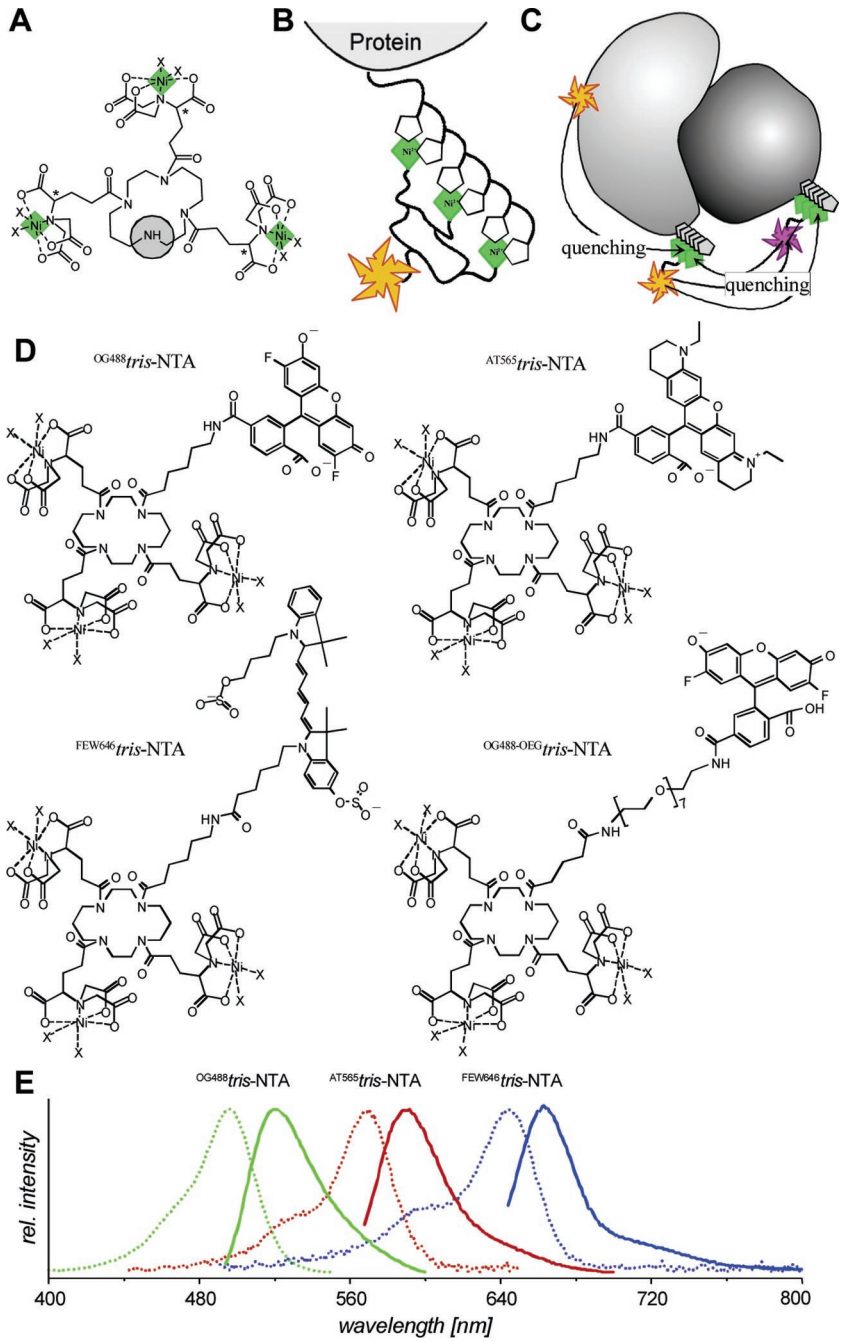

Figure 1. Fluorescence conjugates of tris-NTA for reversible labeling. (A) The chelator head tris-NTA carries three NTA moieties for complexing three Ni(II)-ions (green) and a secondary amino group for conjugation with the fluorophore (gray). (B) Fluorophores conjugated with tris-NTA interact with an oligohistidine-tag by multivalent interaction. (C) Site-specific incorporation of transition metal ions into the protein by tris-NTA provides an additional spectroscopic readout for protein−protein interactions based on fluorescence quenching. (D) Chemical structures of the tris-NTA/fluorophore conjugates ^{OG488}tris-NTA, ^{AT565}tris-NTA, ^{FEW646}tris-NTA, and $^{OG488-OEG}$tris-NTA. Charges at the chelator heads are omitted, and additional ligands coordinated by the chelated Ni(II) ions are denoted by X. (E) Absorption (---) and emission (−−) spectra of ^{OG488}tris-NTA, ^{AT565}tris-NTA, and ^{FEW646}tris-NTA.

achieved because biological high-affinity recognition used for stable fluorophore attachment cannot be dissociated under mild conditions. Furthermore, small entities for highly defined localization of fluorescence dyes within the labeled protein are advantageous for probing protein−protein interactions by fluorescence techniques such as fluorescence resonance energy transfer (FRET).[8]

Using multivalency as a design principle, we have engineered a chemical recognition unit with exceptionally high affinity for oligohistidine tagged proteins.[23] Three nitrilotriacetic acid (NTA) moieties were grafted on a cyclic scaffold to form tris-NTA, which contained an additional functional group for coupling different fluorophores (Figure 1A). Tris-NTA potentially coordinates six imidazole moieties and thus perfectly matches the coordination demands of a hexahistidine-tag (Figure 1B). An additional spectroscopic readout for interaction analysis is provided by the incorporation of three (paramagnetic) transition metal ions into proteins, which potentially quench proximal fluorophores (Figure 1C).[24,25] mono-NTA and tris-NTA were conjugated with Oregon Green 488 (^{OG488}mono-NTA and

(23) Lata, S.; Reichel, A.; Brock, R.; Tampé, R.; Piehler, J. *J. Am. Chem. Soc.* **2005**, *127*, 10205−10215.

^{OG488}tris-NTA, respectively) to demonstrate stable labeling by multivalent interaction. The effect of increasing the distance between the tris-NTA headgroup and the fluorescence dye on the photophysical properties was investigated by incorporating a long, flexible heptaethylene glycol spacer (OG488-OEGtris-NTA). Tris-NTA was furthermore conjugated to ATTO 565 (AT565tris-NTA) and the Cy5-analogue FEW S0387 (FEW-646tris-NTA) (Figure 1D). These dyes cover the visible spectral range (Figure 2E) and are well-compatible with standard microscope equipment. Good spectral overlap furthermore provides a potential application as FRET pairs. We demonstrate stable, site-specific, and stoichiometric fluorescence labeling by tris-NTA/fluorophore conjugates even in cell lysates and on cell surfaces, which was employed for dissecting ligand-mediated cross-linking of the subunits of the type I interferon receptor in solution and on surfaces.

Materials and Methods

Synthesis. The multivalent chelator tris-NTA and its fluorophore conjugates were synthesized as described in detail in the Supporting Information. Briefly, *t*-butyl-protected tris-NTA was obtained by coupling three carboxyl-functionalized NTA moieties to the imino groups of a cyclam scaffold. To the fourth imino group of the cyclam, an amino caproic acid spacer was coupled. After removing all the protection groups in a single step with TFA, the fluorophores were coupled to the primary amino group of the amino caproic acid spacer. Commercially available NHS active esters of Oregon Green 488 (Molecular Probes, Eugene, OR), ATTO 565 (ATTO-TEC GmbH, Siegen, Germany), and FEW S0387 (FEW Chemical GmbH, Wolfen, Germany) were used. The products were purified by preparative thin-layer chromatography to remove nonreacted tris-NTA. After incubating with a stoichiometric excess of nickel(II) chloride, the conjugates were loaded onto a anion exchange column (HiTrap Q, Amersham Biosciences) and eluted with a gradient of 0−500 mM sodium chloride.

Protein Expression and Purification. Ifnar2-H6, ifnar2-H10, and IFNα2 were expressed in *Escherichia coli*, refolded from inclusion bodies, and purified by anion exchange and size exclusion chromatography as previously described.[26] IFNα2 S136C was expressed and site-specifically labeled with Alexa Fluor 488 (^{AF488}IFNα2) as previously reported.[27] An IFNα2 variant with nanomolar affinity toward ifnar1[28] was labeled with Oregon Green 488 maleimide (Molecular Probes, Eugene, OR) in the same manner (^{OG488}IFNα2). Ifnar1-H10 and H10-ifnar1 were expressed in *Sf9* insect cells using the baculovirus system (BaculoGold, BD Biosciences) and purified to homogeneity from the supernatant as previously described.[29,30] MBP-H6 and MBP-H10 were expressed, purified, and labeled with Oregon Green 488 NHS ester with a labeling degree of ∼1 according to standard protocols (^{OG488}MBP-H6 and ^{OG488}MBP-H10, respectively).[31]

Binding Constants. The kinetics of the interaction of ^{OG488}mono-NTA and ^{OG488}tris-NTA with ^{OG488}MBP-H6 and ^{OG488}MBP-H10 was studied by monitoring fluorescence quenching upon complex formation. This method was previously employed using fluorescein-conjugated oligohistidine-peptides.[23] Fluorescence changes due to metal-ion mediated quenching (cf. Figure 1) were monitored at a 5 μM concentration of each interaction partner by stopped-flow fluorescence detection (π* 180 CDF, Applied Photophysics). Fluorescence quenching during dissociation of the complex (1 μM of each interaction partner) upon the addition of 10 μM unlabeled MBP-H10 was measured by stopped-low fluorescence detection for mono-NTA and in a cuvette of a

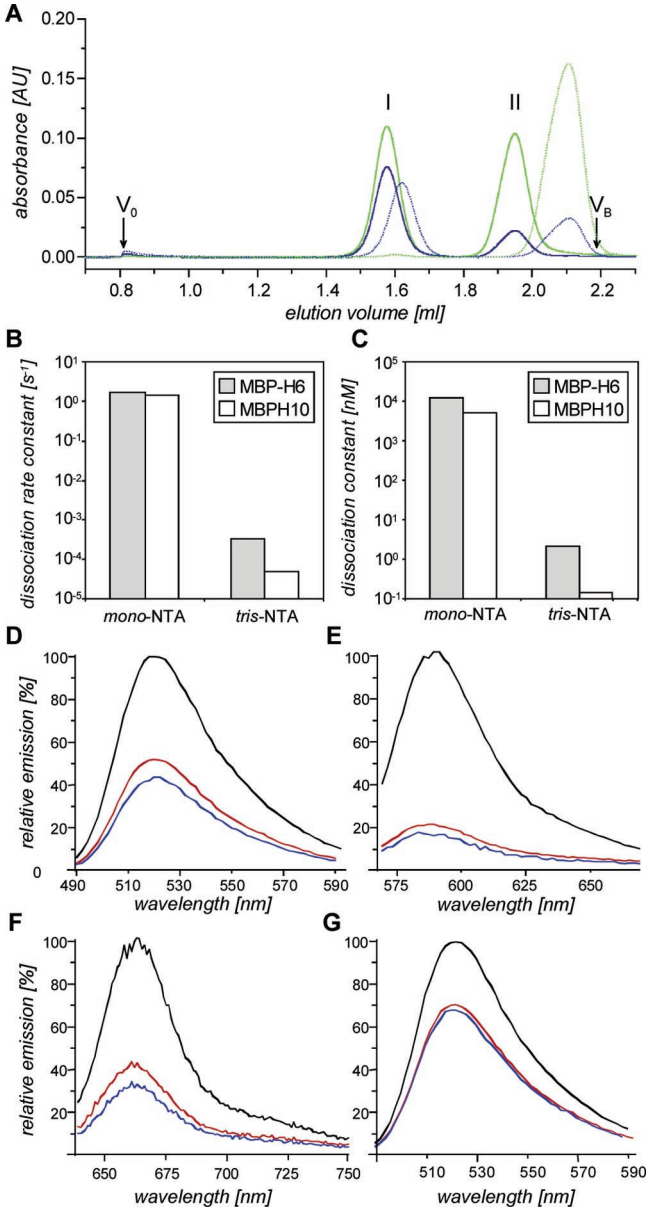

Figure 2. Stable attachment of fluorophores by tris-NTA but not mono-NTA. (A) Analytical SEC of ifnar2-H6 incubated with a 1-fold excess of ^{OG488}mono-NTA (dotted line) and ^{OG488}tris-NTA (solid line). Elution was monitored at 280 nm (blue) and 490 nm (green). The peaks obtained for the protein and the free conjugate are marked with I and II, respectively. The exclusion volume V_0 and the bed volume V_B are indicated by arrows. Identical labeling efficiencies and complex stabilities as for ^{OG488}tris-NTA were obtained for ^{AT565}tris-NTA and for ^{FEW646}tris-NTA. (B) Dissociation rate constant determined for the interaction of mono-NTA and tris-NTA with MBP-H6 and MBP-H10 by monitoring fluorescence dequenching. (C) Equilibrium dissociation constants calculated from the association and dissociation rate constants, which were determined by time-resolved fluorescence measurements using ^{OG488}MBP-H10 and ^{OG488}MBP-H6. Fluorescence emission spectra of ^{OG488}tris-NTA (D), ^{AT565}tris-NTA (E), FEW646tris-NTA (F), and OG488-OEGtris-NTA (G). Spectra are shown for the conjugates loaded with Ni(II) ions (red), after attachment to ifnar2-H10 (blue), and after removing the Ni(II) ions with EDTA (black).

(24) Hutschenreiter, S.; Neumann, L.; Radler, U.; Schmitt, L.; Tampe, R. *Chembiochem* **2003**, *4*, 1340−1344.
(25) Fabbrizzi, L.; Licchelli, M.; Pallavicini, P.; Sacchi, D.; Taglietti, A. *Analyst* **1996**, *121*, 1763−1768.
(26) Piehler, J.; Schreiber, G. *J. Mol. Biol.* **1999**, *289*, 57−67.
(27) Gavutis, M.; Lata, S.; Lamken, P.; Müller, P.; Piehler, J. *Biophys. J.* **2005**, *88*, 4289−4302.
(28) Jaitin, D.; Roisman, L. C.; Jaks, E.; Gavutis, M.; Piehler, J.; Van der Heyden, J.; Uze, G.; Schreiber, G. *Mol. Cell Biol.* **2005**, in press.
(29) Lamken, P.; Lata, S.; Gavutis, M.; Piehler, J. *J. Mol. Biol.* **2004**, *341*, 303−318.
(30) Lamken, P.; Gavutis, M.; Peters, I.; Van der Heyden, J.; Uze, G.; Piehler, J. *J. Mol. Biol* **2005**, *350*, 476−488.
(31) Lata, S.; Piehler, J. *Anal.Chem.* **2005**, *77*, 1096−1105.

fluorescence spectrometer (Cary Eclipse, Varian) for tris-NTA. The fluorescence dequenching upon exchange of the complex was converted into a relative change for comparison of different pairs. Equilibrium dissociation constants were determined from association and dissociation rate constants.

Size Exclusion Chromatography. For preparative protein labeling, olighistidine tagged proteins (10−20 μM) were incubated with a 1.5-fold molar excess of a given tris-NTA/fluorophore conjugate in 20 mM HEPES pH 7.5 and 150 mM NaCl (HBS) for 20 min, followed by size exclusion chromatography (Superdex 200 HR10/30) in an Äkta Prime system (Amersham Biosciences) with a sample volume of 500 μL. The analytical size exclusion chromatography was carried out using a Superdex 200 PC 3.2/30 column in a SMART system (Amersham Biosciences). A total of 50 μL of the sample was injected, and elution was monitored at 280, 490, and 600 nm at a constant flow rate of 50−100 μL/min.

Fluorescence Spectroscopy. The fluorescence spectra of tris-NTA/fluorophore conjugates loaded with Ni^{2+}-ions were recorded in a Cary Eclipse fluorescence spectrometer (Varian) at excitation wavelengths of 470 nm for OG488, 540 nm for AT565, and 620 nm for FEW646. For quantifying the quenching of the conjugates by coordinating Ni(II) ions, 1 mM EDTA was incubated, and the recovery of the fluorescence was monitored in the spectrofluorimeter until equilibrium. For detection of IFNβ-mediated cross-linking of ifnar1-EC and ifnar2-EC, 500 nM IFNβ was added to a mixture of 500 nM ifnar1-H10 and 500 nM ifnar2-H10 labeled with the respective tris-NTA conjugates, and the emission spectra were monitored using the same excitation wavelengths as reported previously.

Expression in Living Cells and Imaging. Full length ifnar2 with an N-terminal H10-tag was cloned into the vector pACgp67B (BD Biosciences), and a recombinant baculovirus was obtained by cotransfection with linearized baculovirus DNA according to the instructions from the manufacturer (BaculoGold, BD Biosciences). Fresh *Sf*9 cells ($\sim 10^6$) were seeded into each well of a six well plate carrying coverslips and were transfected with the baculovirus after 1 h. Two days after transfection, the coverslips were mounted in a perfusion chamber under HBS. Fluorescence imaging was carried out with a laser-scanning confocal microscope (LSM 510, Carl Zeiss Jena) using a 63× magnification objective. The cells were incubated with 100 nM ^{AF488}IFNα2 and then imaged using the 488 nm line of an argon ion laser for fluorescence excitation and a 515 nm long-pass filter for detection. After extensive washing, the same samples were then stained with ^{FEW656}tris-NTA (100 nM) for 5 min, and the excess dye was washed away. The images were acquired by exciting at 633 nm using a helium−neon laser and detection through a 650 nm long-pass filter. After the addition of imidazole (100 mM), the images were further collected under the same conditions.

Surface Sensitive Detection. Interaction on surfaces was monitored by simultaneous total internal reflection fluorescence spectroscopy and reflectance interference detection as in principles reported earlier.[27] OG488 and FEW646 fluorescence was excited simultaneously with an argon ion laser (488 nm) and a helium−neon laser (633 nm). For protein immobilization, the transducer surface was covered with a PEG polymer brush to prevent nonspecific adsorption, and tris-NTA was covalently attached as described recently.[31] Ifnar2-H10 was immobilized through its C-terminal decahistidine tag, and excess tris-NTA groups were blocked with MBP-H10. Ternary complex formation was studied using ^{OG488}IFNα2. Ifnar1-H10 was labeled by adding a 4-fold molar excess of ^{FEW646}tris-NTA. All binding experiments were carried in HBS buffer using a flow-through system as described.[27]

Results

Stable Fluorophore Attachment by tris-NTA Adapter. Reversible protein labeling with different tris-NTA/fluorophore conjugates was demonstrated using the extracellular domains of the type I interferon receptor subunits ifnar1 (ifnar1-EC) and ifnar2 (ifnar2-EC).[29] Ifnar2-EC with a C-terminal hexa- and a deca-histidine tag (ifnar2-H6 and ifnar2-H10, respectively) and ifnar1-EC with a C-terminal decahistidine tag (ifnar1-H10) were used for this study. We have previously reported improved binding affinities for a fluorescein derivative of tris-NTA as compared to mono-NTA.[23] Stable binding of the tris-NTA conjugates used in this study was confirmed by analytical size exclusion chromatography (SEC), as shown for ^{OG488}tris-NTA in comparison to ^{OG488}mono-NTA in Figure 2A. The protein and amount of dye remaining attached to the protein were discriminated by dual wavelength detection at 280 and 490 nm, respectively (Figure 2A).

While ^{OG488}mono-NTA was hardly detectable in the protein peak, a labeling degree of close to 100% was observed with ^{OG488}tris-NTA. Quantitative labeling was also obtained for ^{AT565}tris-NTA and ^{FEW646}tris-NTA (data not shown). Even with an excess of H10-tagged protein, only 1:1 complexes were observed in SEC, which was also previously confirmed by ITC.[23]

The stability of the chelator−protein complexes was furthermore assessed using OG488-labeled maltose binding protein, which was tagged with H6 (^{OG488}MBP-H6) and H10 (^{OG488}MBP-H10) at the C-terminus. Binding of tris-NTA conjugates to these proteins reduced the OG488 fluorescence by 20−30%, probably by transition metal ion-mediated quenching (cf. Figure 2C). Thus, complex dissociation upon challenging with a 10-fold molar excess of nonlabeled MBP-H10 was detected by monitoring the fluorescence recovery (data not shown). Extremely fast dissociation of the complex was observed for ^{OG488}mono-NTA with both ^{OG488}MBP-H6 as well as ^{OG488}MBP-H10 with dissociation rate constants k_d of $\sim 1\ s^{-1}$. For ^{OG488}tris-NTA, however, dissociation rate constants of 3×10^{-4} and $6 \times 10^{-5}\ s^{-1}$ were obtained with MBP-H6 and MBP-H10, respectively (Figure 2B). Thus, an increase in complex stability by 4 orders of magnitude as compared to mono-NTA was achieved by multivalency. By monitoring fluorescence quenching upon complex formation, association rate constants of $1-5 \times 10^5\ M^{-1}\ s^{-1}$ were obtained for all complexes. The equilibrium dissociation constants K_d determined from association and dissociation rate constants are compared in Figure 2C. Compared to ~ 10 μM obtained for mono-NTA, a subnanomolar K_d was reached for the ^{OG488}tris-NTA/MBP-H10 complex. Strikingly, these rate constants and binding affinities were in good agreement with the binding constants obtained for the interaction with the corresponding histidine-peptides.[23] Despite these high affinities and stabilities of the tris-NTA/oligohistidine complexes, quantitative dissociation within a few seconds was observed upon adding 100 mM imidazole (data not shown). This ability to rapidly switch under mild conditions is a key advantage of multivalent coordinative interaction. The kinetics of removing the tris-NTA conjugates from the histidine-tagged proteins can be adjusted by the imidazole concentration. At 20 mM imidazole, the ^{OG488}tris-NTA/MBP-H6 complexes eluted completely dissociated in analytical SEC.

Photophysical and Biochemical Properties. Fluorophores proximal to metal ions are liable to alteration in their photophysical properties. In particular, paramagnetic transition metal ions have been reported to potently quench fluorescence by

electron and energy transfer.[24,25,32−35] Indeed, substantial increases in fluorescence intensity were observed upon removing the coordinated Ni(II) ions from the tris-NTA conjugates with EDTA (Figure 2D−G). Quenching by ∼50% for ^{OG488}tris-NTA, ∼80% for ^{AT565}tris-NTA, and ∼60% for ^{FEW646}tris-NTA was observed upon loading the NTA moieties with Ni(II) ions (cf. Supporting Information). Binding to the protein further reduced the quantum yield of the fluorophores by another 5−10%. Quenching by coordination of Ni(II) ions was distance-dependent, as significantly lower fluorescence quenching was observed for OG488-OEGtris-NTA upon loading with Ni(II) ions (Figure 3G). While the losses in fluorescence quantum yields were not critical for sensitive fluorescence detection, distance-dependent fluorescence quenching by the incorporated Ni(II) ions added a versatile feature for protein interaction analysis.

Ligand recognition by ifnar2-H10 after labeling with ^{OG488}tris-NTA was studied by analytical SEC. After removing the excess of ^{OG488}tris-NTA by SEC, ^{OG488}tris-NTA-labeled ifnar2-H10 was rechromatographed with and without preincubation with IFNα2 (Figure 3A,B). No free dye was detectable in these chromatograms, confirming stable attachment of the conjugates to the protein. Upon adding the ligand, the peak observed for ifnar2-H10 disappeared, while two new peaks were detected at 280 nm, one representing the complex (at 1.49 mL), the other the excess of IFNα2 (at 1.71 mL). At 490 nm, a single peak was detected (Figure 3B), corresponding to the ^{OG488}tris-NTA-labeled ifnar2-H10/IFNα2 complex. This experiment confirmed that full binding activity of the protein was maintained during labeling with ^{OG488}tris-NTA. Similar results were obtained after labeling with ^{AT565}tris-NTA and with FEW646tris-NTA, corroborating site-specific labeling without affecting protein function (data not shown).

Highly Selective Recognition of Oligohistidine-Tagged Proteins. The selectivity of tris-NTA was explored by labeling ifnar2-H10 with ^{FEW646}tris-NTA in a crude *E. coli* cell lysate as studied by analytical SEC. The elution profile recorded at 280 nm showed an enormous absorption throughout the chromatogram (Figure 3C). In contrast, the chromatogram recorded at 600 nm showed only two distinct peaks at 1.55 and 1.97 mL, which correspond to the elution volumes of ^{FEW646}tris-NTA labeled ifnar2-H10 and the excess ^{FEW646}tris-NTA, respectively. Strikingly, the peak at 1.55 mL detected at 600 nm underwent a quantitative shift to 1.46 mL upon incubation with an excess of IFNα2 (Figure 3D), thus confirming the highly specific labeling of ifnar2-H10 in the crude cell lysate. However, no significant change of the chromatogram recorded at 280 nm was detected upon incubation with IFNα2. This experiment demonstrated the high selectivity of tris-NTA as it requires strongly cumulated histidines for efficient complex formation.

Specific protein labeling by tris-NTA fluorophore conjugates was also achieved in living cells (Figure 4). Sf9 insect cells overexpressing full-length ifnar2 with an N-terminal, extracellular H10-tag were analyzed for ligand binding and reversible labeling with ^{FEW646}tris-NTA using fluorescence microscopy. Binding of ^{AF488}IFNα2 (Figure 4A) was observed for the same set of cells, which were also stained by ^{FEW646}tris-NTA (Figure 4B), and corresponded to the state of infection as estimated from the size of the nuclei. Both ^{AF488}IFNα2 and ^{FEW646}tris-NTA binding was highly specific: no staining by ^{AF488}IFNα2 was observed in the presence of unlabeled IFNα2 (data not shown), and the fluorescence of ^{FEW646}tris-NTA was quantitatively removed upon the addition of 150 mM imidazole (Figure 4C).

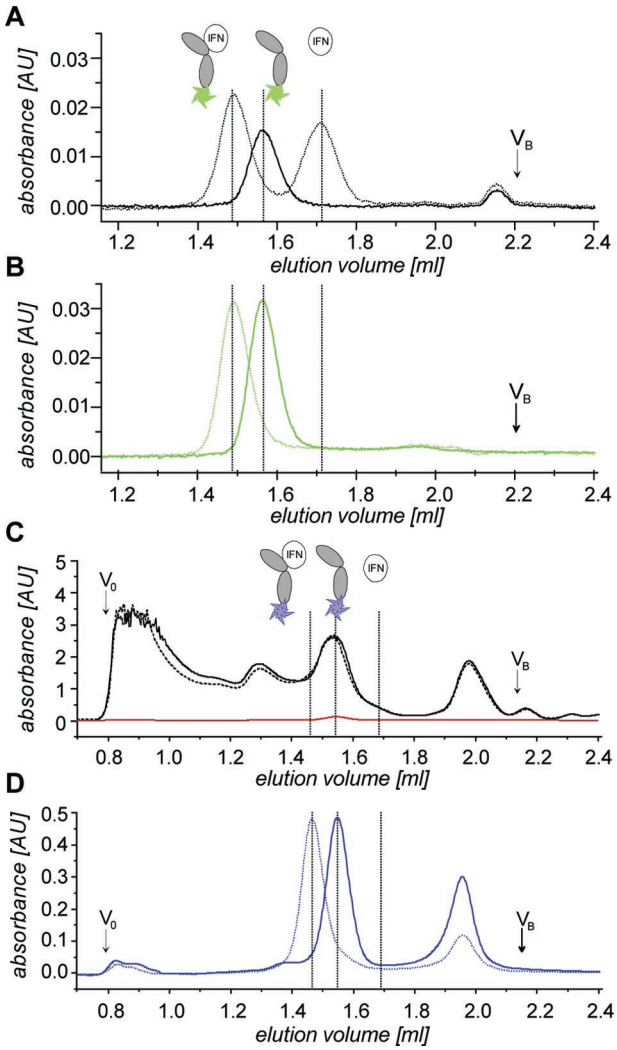

Figure 3. Site-specific and selective labeling of ifnar2-H10 by tris-NTA conjugates. (A and B) Analytical SEC of ^{OG488}tris-NTA-labeled ifnar2-H10 (1 μM) after removing excess ^{OG488}tris-NTA (—). The chromatograms were recorded simultaneously at 280 nm (A) and 490 nm (B). The same sample was incubated with 1.5 μM IFNα2 and chromatographed under the same conditions (·····). (C and D) ^{FEW646}tris-NTA-Mediated labeling of ifnar2-H10 in a cell lysate analyzed by analytical SEC. A crude *E. coli* cell lysate (OD_{280} ∼400 AU) seeded with ifnar2-H10 (10 μM, OD_{280} ∼0.3 AU) was incubated with ^{FEW646}tris-NTA (15 μM) and chromatographed with simultaneous detection at 280 nm (C) and 600 nm (D). When substoichiometric quantities of ^{FEW646}tris-NTA were used, only one peak at 1.55 mL was observed (data not shown). The spectral characteristics of the signal detected in the exclusion volume suggested that it stemmed from scattering and not from nonspecifically bound fluorescence dye. The same experiment was carried out after adding 15 μM IFNα2 (·····).

Detection of Multi-Protein Complex Formation in Solution. Functional analysis of multi-protein complexes is a particular critical task requiring selective spectroscopic readouts. Here, we investigated cross-linking of ifnar1-EC and ifnar2-EC by its ligand IFNβ by analytical SEC and by fluorescence spectroscopy by making use of the versatile labeling and

(32) Varnes, A. W.; Wehry, E. L.; Dodson, R. B. *J. Am. Chem. Soc.* **1972**, *94*, 946−950.
(33) Masuhara, H.; Shioyama, H.; Saito, T.; Hamada, K.; Yasoshima, S.; Mataga, N. *J. Phys. Chem.* **1984**, *88*, 5868−5873.
(34) Richmond, T. A.; Takahashi, T. T.; Shimkhada, R.; Bernsdorf, J. *Biochem. Biophys. Res. Commun.* **2000**, *268*, 462−465.
(35) Rurack, K. *Spectrochim. Acta, Part A* **2001**, *57*, 2161−2195.

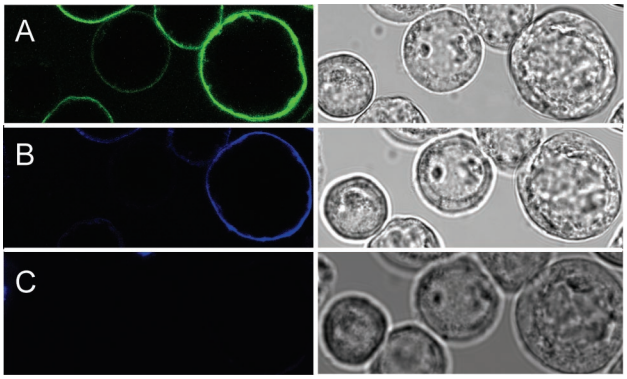

Figure 4. Labeling of full-length ifnar2 in the plasma membrane of living cells. Confocal fluorescence (left panels) and transmission (right panels) images of Sf9 cells expressing full length ifnar2 tagged with H10 at the N-terminus. (A) Image obtained on the green fluorescence channel (488 nm excitation) after staining with 100 nM ^{AF488}IFNα2. (B) Image obtained on the red fluorescence channel after staining the same cells subsequently with ^{FEW646}tris-NTA. (C) Image obtained on the red fluorescence channel (633 nm excitation) after incubating the same cells subsequently of 100 mM imidazole.

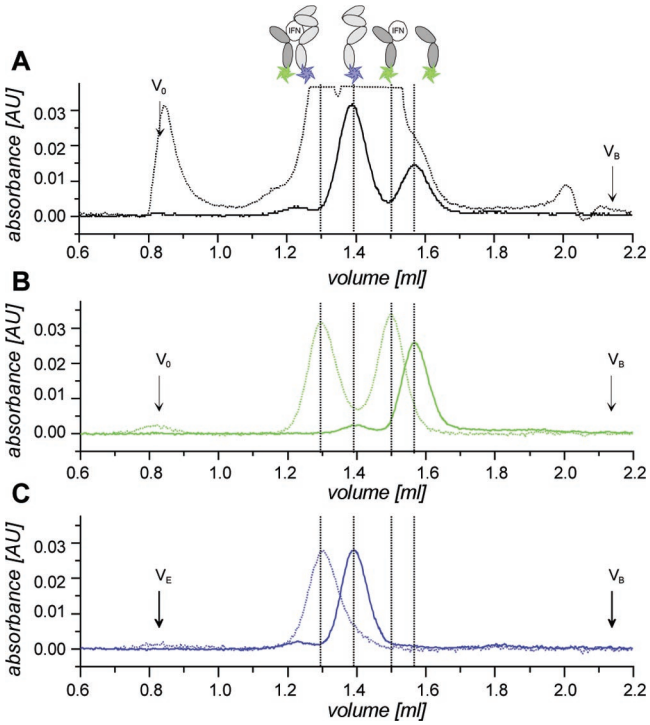

Figure 5. Ternary complex formation of ifnar2-EC and ifnar1-EC with IFNβ as detected by analytical SEC. Ifnar2-H10 and ifnar1-H10 were labeled with ^{OG488}tris-NTA and ^{FEW646}tris-NTA, respectively. ^{OG488}tris-NTA-Labeled ifnar2-H10 and ^{FEW646}tris-NTA-labeled ifnar1-H10 were mixed, and SEC was carried out with detection at 280 nm (A), 490 nm (B), and 600 nm (C) before (·····) and after (—) the addition of IFNβ. The dotted lines mark the elution volumes of ifnar2-H10, of the IFNβ/ifnar2-H10 complex, of ifnar1-H10, and of the ternary complex between ifnar1-H10, ifnar2-H10, and IFNβ.

interaction assays offered by tris-NTA/fluorophore conjugates (Figure 5). Ifnar1-H10 and ifnar2-H10 were labeled with ^{FEW646}tris-NTA and ^{OG488}tris-NTA, respectively, for analyzing ligand-induced cross-linking by analytical SEC (Figure 5A–C). Since the formulated IFNβ used for these experiment contained large quantities of human serum albumin (HSA), no conclusive chromatograms were recorded with detection at 280 nm after adding the ligand (Figure 5A). In contrast, the

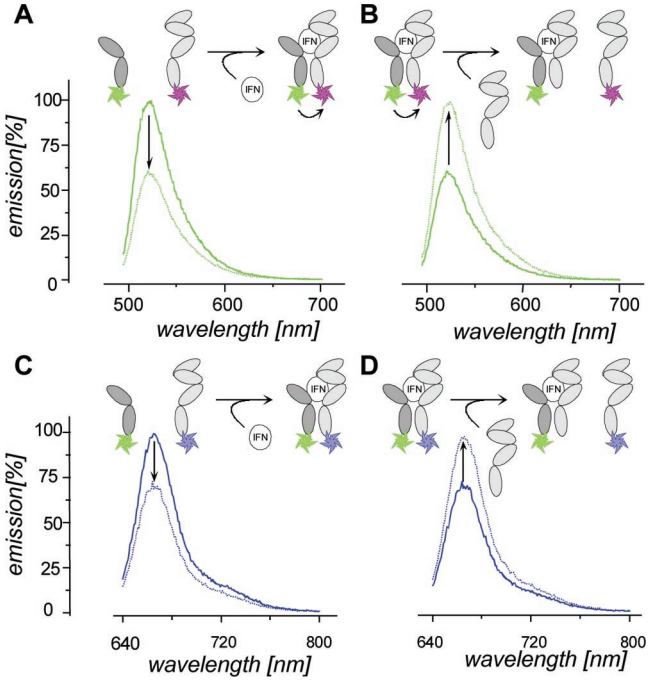

Figure 6. Detection of ligand-induced cross-linking by fluorescence spectroscopy. (A) Fluorescence quenching between the receptor subunits upon ligand binding. Left panel: emission spectra (excitation at 470 nm) of an equimolar (500 nM) solution of ^{OG488}tris-NTA-labeled ifnar2-H10 and ^{AT565}tris-NTA-labeled ifnar1-H10 with (·····) and without (—) incubation with IFNβ (500 nM). (B) Emission spectra (excitation at 470 nm) of ^{OG488}tris-NTA-labeled ifnar2-H10 and ^{AT565}tris-NTA-labeled ifnar1-H10 before (—) and after (·····) the addition of 10-fold molar excess of nonlabeled ifnar1-H10. (C and D) The same experiment as shown in panels A and B carried out with ^{FEW646}tris-NTA-labeled ifnar1-H10 instead of ^{AT565}tris-NTA-labeled ifnar1-H10. In this case, the fluorescence of FEW646 was recorded (excitation at 620 nm).

chromatograms recorded at 490 nm (Figure 5B) and 600 nm (Figure 5C) showed a clear peak at 1.39 mL, confirming that both ifnar2-EC and ifnar1-EC were involved in the ternary complex. Taking into account the elution volumes and absorption at 490 and 600 nm, the peak observed at 1.30 mL can be conclusively assigned to a ternary complex (1:1:1) between ifnar1-H10, ifnar2-H10, and IFNβ. The second peak selectively detected at 490 nm (1.49 mL) corresponds to a binary complex (1:1) between ifnar2-H10 and IFNβ.

To monitor ternary complex formation, ^{OG488}tris-NTA-labeled ifnar1-H10 and ^{AT565}tris-NTA-labeled ifnar1-H10 were cross-linked at stoichiometric ratios by the addition of IFNβ while monitoring the fluorescence spectrum upon excitation at 470 nm.

A drop in fluorescence intensity of ~40% was observed at 515 nm after adding the ligand (Figure 6A), suggesting FRET due to an increased proximity of the receptor subunits in the ternary complex. Indeed, the fluorescence intensity recovered to its original value when the labeled ifnar1-H10 was competed out with a 10-fold molar excess of the unlabeled ifnar1-H10 (Figure 6B). However, no sensitized fluorescence was detectable in this assay, suggesting that changes in fluorescence intensity were at least partially due to Ni(II) ion-mediated quenching. Therefore, the same binding assay was carried out with ifnar1-H10 labeled with ^{FEW646}tris-NTA instead of ^{AT565}tris-NTA. Thus, spectral overlap with the emission spectrum of OG488 was minimized. After the addition of a stoichiometric amount of IFNβ, the fluorescence of FEW646 was measured. Under these

conditions, contribution by FRET to the fluorescence quenching was negligible. Yet, substantial fluorescence quenching of ^{EW646}tris-NTA was observed upon IFNβ-induced cross-linking of the receptor subunits (~30%, Figure 6C), which was fully reversed upon adding unlabeled ifnar1-H10 (Figure 6D). For other cytokine receptors, close proximity of the C-terminal domains has been observed in the ligand−receptor complexes,[36,37] which is probably also the case for ifnar. This could explain the strong quenching effect observed in these assays. However, transition metal ion mediated fluorescence quenching proved to be a powerful feature of tris-NTA based fluorescence labeling for sensitive detection of protein interactions in solution.

Protein Complex Formation on Surfaces. Noncovalent labeling through tris-NTA was furthermore employed for studying ternary complex formation on surfaces by simultaneous surface-sensitive fluorescence detection by total internal reflection fluorescence spectroscopy (TIRFS) and mass-sensitive detection by reflectance interference (RIf) in real time (Figure 7). Ifnar2-H10 was immobilized using tris-NTA attached to a molecular poly(ethylene glycol) brush,[31] and the excess of tris-NTA groups on the surface was blocked with MBP-H10. Fluorescence and RIf signals during a typical sequence of injections are shown in Figure 7B: when ifnar1-EC with an N-terminal decahistidine-tag (H10-ifnar1) labeled with ^{FEW646}tris-NTA was injected, a transient signal on the red fluorescence channel was observed, which can be ascribed to background fluorescence excitation. Upon injection of ^{FEW646}tris-NTA-labeled H10-ifnar1 in the presence of ^{OG488}IFNα2, protein binding was detected on both fluorescence channels, indicating ternary complex formation on the surface. Protein binding was also detectable by mass-sensitive RIf detection. During the injection of ^{OG488}IFNα2 alone, a response was detectable on the green fluorescence channel, as well as by RIf. While the same amplitude of the fluorescence signal was detected as during the preceding injection, the mass signal was substantially lower, confirming that indeed a ternary complex was formed. The normalized signals detected during the second injections are compared in Figure 7C. While similar association kinetics was observed on all three channels, the decay of the red fluorescence signal was significantly faster than the decay of the green fluorescence, in agreement with the faster dissociation of ifnar1-EC from ^{OG488}IFNα2 (k_d ~0.05 s^{-1}) than the dissociation of ^{OG488}IFNα2 from ifnar2-H10 (k_d ~0.025 s^{-1}). By fitting corresponding models to these curves, the same dissociation rate constants were obtained, confirming noncooperative interaction of ifnar1-EC and ifnar2-EC with IFNα2. The overlay of the green fluorescence signal from the second and the third injection is shown in Figure 7D. Strikingly, both association and dissociation signals overlaid perfectly, corroborating that the interaction H10-ifnar1 with IFNα2 does not affect its interaction with ifnar2-H10. By fitting a first-order model, the same interaction rate constants were obtained for both binding curves.

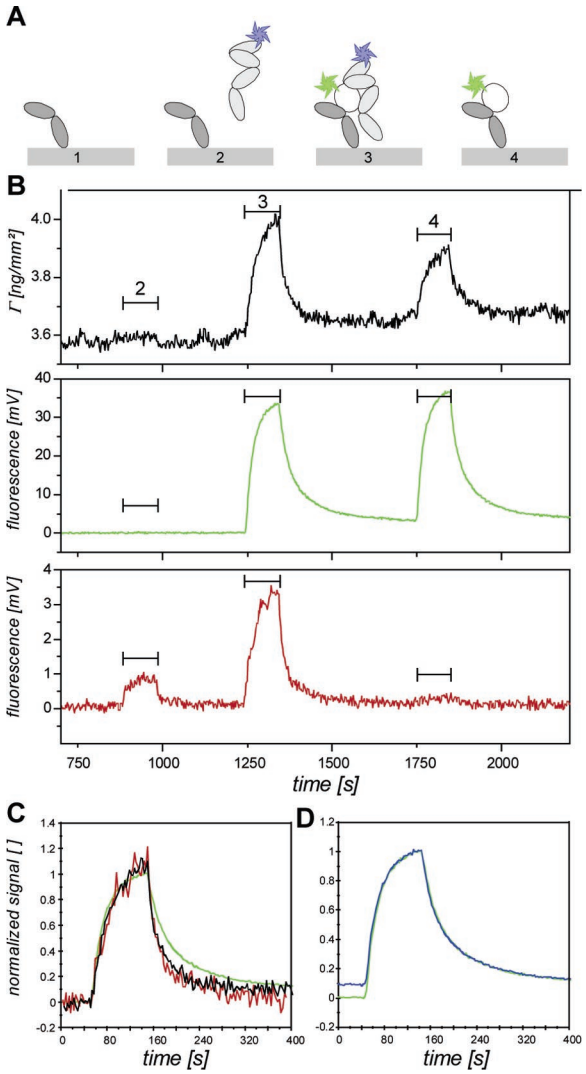

Figure 7. Dissection of multi-protein complex formation by surface-sensitive detection. (A) Schematic of the binding assays: after immobilization of ifnar2-H10 (1), first H10-ifnar1-labeled with ^{FEW646}tris-NTA was injected (2), then the complex of H10-ifnar1/^{FEW646}tris-NTA with ^{OG488}IFNα2 (3), and then ^{OG488}IFNα2 alone (4). (B) Typical binding curves as detected by simultaneous TIRFS-RIf detection upon sequential injection of 200 nM H10-ifnar1 with 800 nM ^{FEW646}tris-NTA (I), 200 nM H10-ifnar1 with 800 nM ^{FEW646}tris-NTA and 100 nM ^{OG488}IFNα2 (II), and 100 nM ^{OG488}IFNα2 (II): mass signal (black), green fluorescence (green), and red fluorescence (red). (C) Overlay of the three signals during injection II normalized to the maximum signal (same color coding as panel B). (D) Overlay of the green fluorescence signal during injection II (green) and injection III (blue), normalized to the maximum signal.

Discussion

Stable, yet reversible fluorescence labeling of recombinant proteins is a challenging task because high-affinity recognition such as streptavidin−biotin interaction can only be reversed under very drastic conditions. Here, we employed a chemical adaptor, which binds histidine-tagged proteins with subnanomolar affinity by multivalent coordinative interaction. Stable binding of tris-NTA requires cumulated oligo-histidines, thus making possible selective labeling of proteins in complex matrixes and on the surface of living cells. In contrast to high-affinity recognition by proteins, the degenerate multivalent interaction enables for rapidly reversing the interaction by a monovalent competitor.[38] Thus, the tris-NTA/fluorophore conjugates attached to proteins could be removed by imidazole at millimolar concentrations (i.e., under very mild and physiologi-

(36) de Vos, A. M.; Ultsch, M.; Kossiakoff, A. A. *Science* **1992**, *255*, 306−312.
(37) Syed, R. S.; Reid, S. W.; Li, C.; Cheetham, J. C.; Aoki, K. H.; Liu, B.; Zhan, H.; Osslund, T. D.; Chirino, A. J.; Zhang, J. et al. *Nature* **1998**, *395*, 511−516.
(38) Rao, J.; Lahiri, J.; Isaacs, L.; Weis, R. M.; Whitesides, G. M. *Science* **1998**, *280*, 708−711.

cal conditions), which could even be applied to living cells. This possibility adds powerful features for the application in fluorescence spectroscopy and microscopy as it enables to in situ remove fluorophores attached to the proteins (e.g., for a control experiment), replenish with fresh fluorophore (e.g., after photobleaching), or exchange against a different fluorophore. Owing to the chemical nature of the recognition unit and its relatively small size, the position of the fluorophore within the protein is well-defined as compared to labeling techniques based on autofluorescent proteins or other protein-based labeling techniques.[8] Because of the flexibility of the recognition unit, the labeling of oligohistidine sequences within proteins is likely to be feasible with a similar affinity as observed for the C-terminal histidine-tag. Further interesting features of the tris-NTA fluorophore conjugates result from the site-specific and stoichiometrically defined incorporation of (paramagnetic) transition metal ions into the protein together with the fluorophore. These can be used as probes for different spectroscopic applications including magnetic resonance techniques. Here, we demonstrated that potent fluorescence quenching by Ni(II)-ions incorporated by tris-NTA can be used as a sensitive reporter for protein−protein interactions. Thus, tris-NTA-mediated fluorescence labeling provides not only means for monitoring protein interactions and conformational changes in real-time but also an assessment of inter- and intramolecular distances. Although Ni(II) ion-mediated quenching is assumed to be based on electron transfer, we could observe quenching over rather long distances, as the histidine tags of the two receptor subunits in the ternary complex are probably several nanometers apart. Our observations suggest that other mechanisms than electron transfer may be involved in this quenching process, which remains to be investigated in more detail. A rigorous analysis of the distance-dependence of this quenching effect would enable for quantitative measurements of distances in protein complexes.

Noncovalent fluorescence labeling was also shown to be compatible with surface-sensitive fluorescence detection, which enables for versatile interaction assays. On the basis of multicolor labeling experiments, we could demonstrate noncooperative ternary complex formation of the two receptor subunits of the type I interferon receptor with its ligand. The dissection of multi-protein complex formation is a key challenge for understanding cellular proteom function, and versatile labeling techniques and interaction assays are demanded. We have demonstrated how the tris-NTA fluorophore can be used for studying the composition of protein complexes in complex sample matrixes and for monitoring multi-protein complex formation. Given the enormous prevalence of the histidine-tag for purification of recombinant proteins and its compatibility with all expression systems, broad applications of tris-NTA conjugates in protein interaction analysis can be envisioned.

Acknowledgment. Formulated IFNβ (formulated Rebif) was supplied from Dr. Garth Virgin (Serono GmbH, Gemany). The plasmids for expression of IFNα2 and its variants were provided by Dr. Gideon Schreiber, Weizmann Institute of Science. We thank Gerhard Spatz-Kümbel for excellent technical assistance in organic synthesis, Dirk Paterok and Peter Lamken for ifnar constructs, and Eva Jaks for fluorescence-labeled IFNα2. This work was supported by the DFG (Pi-405/1, Pi-405/2, and Ta-157/6) and by the BMBF (0312005A).

Supporting Information Available: Detailed description of the synthesis, purification, and spectroscopic characterization of the tris-NTA conjugates and a table summarizing the photophysical properties of the tris-NTA/fluorophore conjugates. This material is available free of charge via the Internet at http://pubs.acs.org.

JA0563105